In Exocrine Pancreas, the Basolateral Endocytic Pathway Converges with the Autophagic Pathway Immediately After the Early Endosome

John Tooze,* M. Hollinshead,* T. Ludwig,* K. Howell,‡ B. Hoflack,* and H. Kern§

*European Molecular Biology Laboratory, 6900 Heidelberg, Federal Republic of Germany; ‡University of Colorado Medical School, Denver, Colorado 80262; and §Philipps University Marburg, 3550 Marburg, Federal Republic of Germany

Abstract. Intracisternal granules (ICGs) are insoluble aggregates of pancreatic digestive enzymes and proenzymes that develop within the lumen of the rough endoplasmic reticulum of exocrine pancreatic cells, especially in guinea pigs. These ICGs are eliminated by autophagy. By morphological criteria, we identified three distinct and sequential classes of autophagic compartments, which we refer to as phagophores, Type I autophagic vacuoles, and Type II autophagic vacuoles.

Lobules of guinea pig pancreas were incubated in media containing HRP for periods of 5–120 min to determine the relationship between the endocytic and autophagic pathways. Incubations with HRP of 15 min or less labeled early endosomes at the cell periphery that were not involved in autophagy of ICGs, but after these short incubations none of the autophagic compartments were HRP positive. After 30-min incubation with HRP, early endosomes at the cell periphery, late endosomes in the pericentriolar region, and, in addition, Type I autophagic vacuoles containing ICGs were all labeled by the tracer. Type II autophagic vacuoles were not labeled after 30-min incubation with HRP but were labeled after incubations of 60–120 min. Phagophores did not receive HRP even after 120 min incubations. We concluded that the autophagic and endocytic pathways converge immediately after the early endosome level and that Type I autophagic vacuoles precede Type II autophagic vacuoles on the endocytic pathway.

We studied the distribution of acid phosphatase, lysosomal proteases and cation-independent-mannose-6-phosphate receptor (CI-M6PR) in the three classes of autophagic compartments by histochemical and immunocytochemical methods. Phagophores, the earliest autophagic compartment, contained none of these markers. Type I autophagic vacuoles contained acid phosphatase but, at most, only very low levels of cathepsin D and CI-M6PR. Type II autophagic vacuoles, by contrast, are enriched for acid phosphatase, cathepsin D, and other lysosomal enzymes, and they are also enriched for CI-M6PR. Moreover, soluble fragments of bovine CI-M6PR conjugated to colloidal gold particles heavily labeled Type II but not Type I autophagic vacuoles, and this labeling was specifically blocked by mannose-6-phosphate. This indicates that the lysosomal enzymes present in Type II autophagic vacuoles carry mannose-6-phosphate monoester residues. Using 3-C2, 4-dinitroanilino-3'-amino-N-methyldipropylamine (DAMP), we showed that Type II autophagic vacuoles are acidic. We interpret these findings as indicating that Type II autophagic vacuoles are a prelysosomal compartment in which the already combined endocytic and autophagic pathways meet the delivery pathway of lysosomal enzymes.

COMPARED to the endocytic pathway (Gruenberg and Howell, 1989) and the pathway of delivery of lysosomal enzymes (Kornfeld and Mellman, 1989), the autophagic pathway in animal cells remains poorly characterized (Pfeifer, 1987; Seglen, 1987). Morphological evidence indicates that the first event in autophagy is the sequestration of parts of the cytoplasm, including organelles, within a membrane. The classical view is that this structure then fuses with a lysosome to yield a secondary lysosome containing hydrolases responsible for the degradation of the autophaged cytoplasm. However recent experiments by Gordon and Seglen (1988) and by Steinberg et al. (1988), involving the introduction into the cytosol of marker molecules, imply that the autophagic pathway may meet the endocytic pathway at an earlier, prelysosomal level. Gordon and Seglen (1988) proposed the name amphisome for a compartment containing endocytosed and autophagically sequestered molecules but lacking the lysosomal marker enzyme β glucuronidase.

To investigate further the earliest point of convergence of

the autophagic and endocytic pathways, we have taken advantage of the phenomenon of the formation of intracisternal granules (ICGs)[1] in guinea pig exocrine pancreatic cells. ICGs form spontaneously in a small percentage of exocrine cells in guinea pig pancreas (Palade, 1956), and, albeit more rarely, in exocrine pancreatic cells of other species (Geuze and Slot, 1980). In the guinea pig, very large numbers of ICGs can be induced in virtually every exocrine pancreatic cell by injecting the animals with $CoCl_2$ (Kern and Kern, 1969). Recently, we established that ICGs are insoluble aggregates of the set of pancreatic digestive enzymes and proenzymes held together by intermolecular disulphide bonds (Tooze et al., 1989).

Pancreatic secretory proteins normally traverse the exocytic pathway to be secreted via zymogen granules into the ducts of the acini. When, however, they become trapped in ICGs within the lumen of the rough ER (RER) they cannot move further down the exocytic pathway. Instead, they are eliminated by autophagy; this means that a massive induction of autophagy is a secondary consequence of the induction of ICGs (Kern and Kern, 1969). Whereas, in normal pancreas autophagic vacuoles are infrequently seen in thin sections under the electron microscope (Novikoff et al., 1977), following induction of ICGs they become a very prominent intracellular compartment (Kern and Kern, 1969), which can readily be identified because of the presence of ICGs that are otherwise found only in the RER. Our data indicate that during the autophagy of ICGs in guinea pig exocrine pancreatic cells the endocytic and autophagic pathways converge immediately after the first compartment in each pathway, respectively early endosomes and phagophores. The combined pathways then reach an acidic prelysosomal compartment in which endocytosed and autophaged proteins are colocalized with cation independent mannose-6-phosphate receptor (CI-M6PR) and lysosomal hydrolases, some of which still retain mannose-6-phosphate monoester residues.

Materials and Methods

Induction of ICGs

Young guinea pigs weighing 200–250 g (Charles River Vega GmbH, Sulzfeld, FRG) were injected subcutaneously with $CoCl_2$ in 0.9% sterile saline at a dose of 15 mg/kg body weight at the same time on three consecutive days. The animals were killed by a blow on the head 24 h after the last injection of $CoCl_2$. The pancreas was removed and lobules were prepared. For controls, pancreatic lobules were prepared from normal guinea pigs.

Electron Microscopy

For conventional electron microscopy, freshly dissected pancreatic lobules were fixed at room temperature for 1 h in 1% glutaraldehyde in 0.2 M sodium cacodylate buffer, pH 7.4. They were then given three 10-min washes in 0.2 M sodium cacodylate buffer, pH 7.4, and postfixed in 1% OsO_4 in 0.2 M cacodylate buffer (pH 7.4) for 1 h. After three additional washes in the buffer, the tissue was incubated overnight at 4°C in 0.5% magnesium uranyl acetate (BDH Chemicals Ltd. Poole, England) in water. It was then dehydrated in ethanol and embedded in Epon.

For cryoimmunoelectron microscopy, fresh pancreatic lobules were fixed

for 15–20 min at 4°C in 4% paraformaldehyde in 250 mM Hepes (pH 7.4) and then transferred into 8% paraformaldehyde in Hepes at room temperature for at least 1 h. They were then washed in Hepes, infiltrated with sucrose, and frozen in liquid nitrogen; thin sections of frozen cells were cut and labeled according to published procedures (Tokuyasu, 1980; Griffiths et al., 1984).

3-C2, 4-Dinitroanilino-3'-Amino-N-Methyldipropylamine (DAMP) Labeling

We followed published procedures (Anderson et al., 1984; Anderson and Pathak, 1985) and used immunogold labeling to detect the DAMP. We are grateful to R. G. W. Anderson (University of Texas Health Sciences Center, Dallas, TX) for generously giving us DAMP and anti-DAMP antibody.

Acid Phosphate Cytochemistry

Tissue blocks were fixed in 1% glutaraldehyde for 1 h, and then washed in buffer. Small tissue blocks were then cut and washed for 30 min in buffer containing 10% DMSO (pH 5) used for the cytochemical incubations. To 10 ml of 100 mM buffer (pH 5) plus 10% DMSO, 100 μl of a 12% lead nitrate solution was added, and then, slowly, 1 ml of a 3% solution of β-glycerophosphate. The solution was then filtered and the tissue blocks were incubated at 37°C with agitation for 75 min, changing with fresh solution every 25 min; cytochemical reactions were stopped after this time by washing with buffer, and the blocks then processed for electron microscopy.

Uptake of HRP

Freshly prepared guinea pig pancreatic lobules from experimental and control animals were incubated with oxygenation in flasks in a shaking water bath at 37°C. The medium used was MEM plus 0.1% BSA, 0.01% soybean trypsin inhibitor, and 25 mM Hepes (pH 7.4), and 10 mg/ml HRP (Sigma Type III).

Lobules were removed after 5, 15, 30, 60, 90, and 120 min of incubation and, without washing, immediately fixed in 1.0% glutaraldehyde in 200 mM cacodylate (pH 7.4) for 1 h. The lobules were then washed overnight at 4°C in 200 mM cacodylate (pH 7.4). Small blocks were cut from the fixed, washed lobules, then incubated in 1 mg/ml DAB for 30 min without H_2O_2, and then incubated for 90 min with DAB and H_2O_2. The reaction was then stopped by washing with buffer. The blocks were postfixed in 1% OsO_4 and processed for epon embedding and electron microscopy.

Nocodazole Microtubule Depolymerization

Lobules were excised and kept in incubation medium on ice for 30 min and then for a further 10 min on ice in medium containing 33 μg/ml nocodazole. The lobules were then transferred to 37°C in a shaking water bath into medium containing nocodazole and HRP, 10 mg/ml, while other lobules from the same animal were maintained at 37°C in the absence of nocodazole and transferred into the HRP incubation medium at the same time. At different times up to 90 min, lobules were fixed in 1% glutaraldehyde cacodylate for 1 h. The lobules were then washed in buffer, reacted with DAB, and processed for electron microscopy.

Mannose-6-Phosphate Receptor Fragments Conjugated to Gold

Soluble fragments of mannose-6-phosphate receptor were isolated from bovine serum using a phosphomannan affinity column as described elsewhere (Ludwig, T., G. Griffiths, and B. Hoflack, manuscript submitted for publication). Soluble fragments at a concentration of 300 μg/ml were bound to 9-nm colloidal gold at pH 7.4 at a final concentration of 12 μg/ml gold, and then stabilized by bovine serum albumin at a final concentration of 0.2%. The solution was then concentrated by ultracentrifugation and stored at 4°C.

Thin cryosections were incubated with the M6PR-gold conjugates for 90 min followed by washing. The specificity of the labeling by the soluble fragments was established by incubating sections and receptor–gold conjugates in the presence of 5 mM mannose-6-phosphate. We are very grateful to our colleagues Gareth Griffiths and Ruth Back (EMBL, Heidelberg) for preparing the receptor–gold conjugates.

Immunoblotting CI-M6PR

Pancreas and livers from control and treated guinea pigs were homogenized in 20 ml of ice cold 50 mM Tris/HCl (pH 7.4), 150 mM NaCl, 1 mM EDTA,

---

1. Abbreviations used in this paper: CI-M6PR, cation-independent-mannose-6-phosphate receptor; DAMP, 3-C2, 4-dinitroanilino-3'-amino-N-methydipropylamine; ICG, intracisternal granules; PNS, postnuclear supernatants; RER, rough ER.

containing protease inhibitors (0.1 TIU/ml of aprotinin; 10 μg/ml each of leupeptin, antipain, pepstatin, and chymostatin). Postnuclear supernatants (PNS) were recovered after centrifugation of the homogenates at 1,000 g for 10 min. Proteins were determined according to Bradford (1976). Proteins of the different PNS were separated on a 7.5% SDS-polyacrylamide gel and blotted onto nitrocellulose by the Western procedure (Burnette, 1981). The CI-M6PR was detected with a polyclonal antibody against the bovine CI-M6PR used at a dilution of 1 to 250.

Antibodies

We used the following antibodies for immunogold labeling: (a) rabbit antiserum, and affinity purified antibody raised against bovine liver and rat liver cathepsin D; (b) rabbit antibody against rat cathepsin B, kindly provided by H. Kirschke (University of Halle-Wittenberg, GDR); (c) rabbit antiserum against human acid phosphatase kindly provided by K. von Figura (University of Göttingen, FRG); (d) rabbit antisera and affinity-purified antibody raised against two independent preparations of bovine liver CI-M6PR; (e) rabbit antiserum, and affinity-purified antibody, raised against chicken liver CI-M6PR, kindly provided by R. Römisch (EMBL, Heidelberg, FRG); and (f) rabbit antiserum raised against rat CI-M6PR, kindly provided by K. von Figura, and rabbit antibody against rat lgp120, kindly provided by I. Mellman (Yale University, New Haven, CT).

Results

Morphology of Autophagic Vacuoles

In thin sections of glutaraldehyde-fixed, epon-embedded exocrine pancreatic cells from guinea pigs injected with CoCl$_2$, we observed in the electron microscopic three morphologically distinct types of autophagic compartments containing ICGs. Structures resembling the phagophores in liver cells described by Seglen (1987) were present. The phagophores were relatively small spherical or oval compartments comprised of a multilayered osmiophilic smooth membrane usually enclosing a small amount of cytoplasm containing a circular profile of RER. Usually one, but sometime two or three ICGs were enclosed within this RER (Fig. 1, A-C). In contrast to the situation in Type I and Type II autophagic vacuoles (see below), the ICGs within phagophores were invariably enveloped by RER. The morphological integrity of the RER membrane, still studded with ribosomes, is consistent with Seglen's proposal (1987) that phagophores represent the initial sequestration event of autophagy. Examination of electron micrographs of serial sections (not shown) established that phagophores are discrete, small compartments not attached to other organelles. Typically, they had diameters in the range 200–300 nm such that each phagophore was contained within three or four serial sections each about 80-nm thick.

Secondly, there were larger compartments, referred to here as Type I autophagic vacuoles, consisting of compact clusters of several ICGs enclosed by smooth, often multilayered membrane, which by virtue of its morphology and osmiophilia sometimes resembled the membrane around phagophores (Fig. 1, D-F). In most of these structures there was little evidence of cytoplasm, RER, or free ribosomes, but in some cases we observed a still recognizable phagophore within a Type I autophagic vacuole (for example, Fig. 1 F). Micrographs of serial sections (not shown), and images such as Figs. (1 D and F) led us to conclude that phagophores cluster around and fuse with Type I autophagic vacuoles. Finally, there were large autophagic vacuoles with a smooth bounding membrane, which we refer to here as Type II autophagic vacuoles (Figs. 1 G and 4, D-G). Usually several ICGs, no longer individually enveloped by membrane, lay

within the lumen of Type II autophagic vacuoles, which had another very characteristic feature, namely the presence of large amounts of internal membrane often closely packed in parallel arrays (Fig. 1, G-J). Images such as those shown in Fig. 1 (H-J) establish that at least some of this internal membrane is continuous with the bounding membrane. Finally, examination of serial sections (not shown) established unequivocally that Type I and Type II autophagic vacuoles are separate, distinct compartments.

Based solely on morphological criteria, we considered these three classes of autophagic structures to be three sequential stages of autophagy, namely phagophores, the smallest autophagic compartments in which the sequestered cytoplasm retains its morphological integrity, followed by Type I autophagic vacuoles followed by Type II autophagic vacuoles. This interpretation was substantiated by the immunocytochemical labeling for lysosomal proteins and the studies of endocytosis of HRP described below.

Although we used for these studies pancreas from guinea pigs injected with CoCl$_2$ to induce ICGs in virtually every exocrine cell, we also observed the three classes of autophagic compartments described above in the small percentage of pancreatic exocrine cells of normal control guinea pigs in which ICGs develop spontaneously (Palade, 1956). An example of a Type I autophagic vacuole in normal pancreas is shown in Fig. 4 A. We wish to stress that intoxication with CoCl$_2$ simply increases the frequency of the formation of ICGs in the RER.

Acidity of Autophagic Compartments

We incubated pancreatic lobules freshly prepared from experimental guinea pigs in medium containing DAMP (Anderson et al., 1984; Anderson and Pathak, 1985). After fixation and embedding, cryosections were labeled with anti-DAMP antibodies. Phagophores were not labeled (not shown) but both Type I and Type II autophagic vacuoles were labeled (Fig. 2 A) and are therefore acidic compartments. Since the extent of labeling with DAMP of Type II autophagic vacuoles was greater than that of Type I, we concluded that the former are more acidic than the latter.

Autophaged ICGs Contain Chymotrypsinogen

ICGs contain the complete set of pancreatic digestive enzymes and proenzymes cross-linked together by intermolecular disulphide bonds (Tooze et al., 1989). Within the RER, they can be immunolabeled with antibodies against chymotrypsinogen (Geuze and Slot, 1980; Tooze et al., 1989). The ICGs within autophagic compartments also contain immunoreactive chymotrypsinogen (Fig. 2 B). Outside the RER, ICGs occur in these cells only in autophagic compartments. The ICGs therefore provided us with a very convenient morphological marker of the autophagic pathway.

Convergence of Endocytic and Autophagic Pathways

To determine which if any of the three types of autophagic compartments in these cells are also on the endocytic pathway, we allowed exocrine pancreas to endocytose HRP (Marsh et al., 1986) for various periods of time. Guinea pigs, unlike rats, are difficult to maintain under anaesthesia; we, therefore, chose not to irrigate pancreatic ducts of living guinea pigs with HRP solutions, as has been done with rats (Herzog and Reggio, 1980), but, instead we incubated
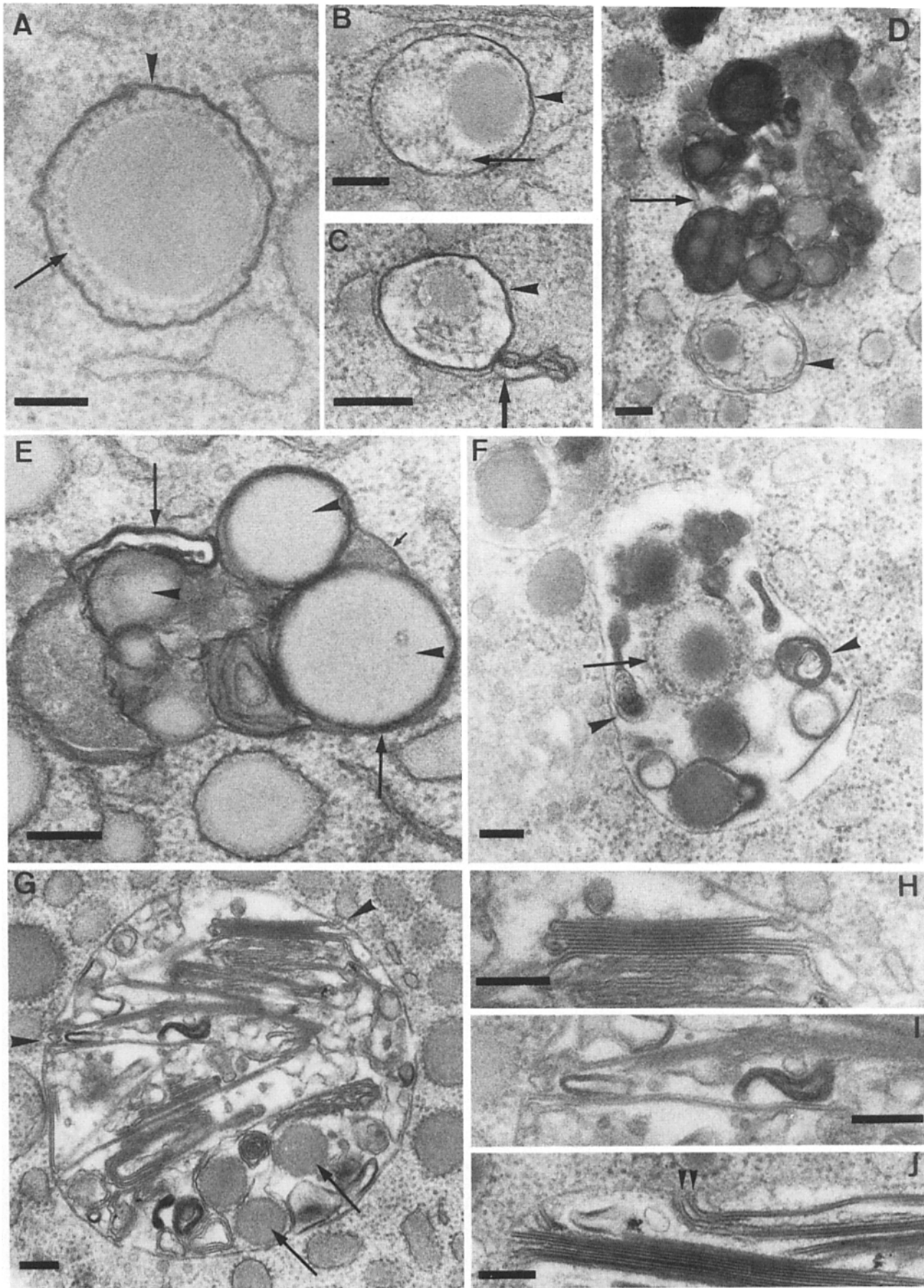
freshly prepared pancreatic lobules from control and experimental animals in oxygenated medium containing 10 mg/ml HRP at 37°C. At various times, the lobules were fixed, processed for the peroxidase reaction, and embedded in epon. In this experimental system the basolateral surfaces of the polarized epithelial exocrine cells of the acini were immediately exposed to the tracer. We found, however, that it took up to 30 min incubation for the HRP to reach by diffusion the lumen of the ducts of the acini and therefore the apical plasma membrane of the exocrine cells. Consequently, at least for the first 15 min, endocytosis was restricted to the basolateral surface.

After 5 min incubation with HRP, a small number of early endosomes close to the basolateral surface were the only compartments labeled in control and experimental lobules (Fig. 3 A). These early endosomes were tubular vesicular structures similar to those seen in other cell types and they did not contain ICGs. By 15 min more early endosomes, still for the most part peripherally located, contained HRP (Fig. 3, B and C). None of the autophagic compartments contained HRP after 15 min incubation and none of the early endosomes with HRP contained ICGs.

After 30 min incubation of control and experimental lobules, the number of HRP positive compartments had increased significantly, and, in addition to peripheral early endosomes, late endosomal compartments close to the centrioles and Golgi apparatus were labeled. Importantly, in the experimental lobules after 30 min incubation with HRP, virtually all of the Type I autophagic vacuoles contained HRP reaction product (Fig. 3, D-G), but both phagophores and Type II autophagic vacuoles were still unlabeled (Fig. 3, E and H).

After 60 min incubation in addition to the labeled compartments seen after 30 min incubation, the lumen of a great majority of the Type II autophagic vacuoles, characterized by the presence of stacked internal membrane and free ICGs, contained HRP reaction product (Fig. 3, I-K). Extending incubations to 90 and 120 min resulted in even heavier labeling of all of the Type II autophagic vacuoles. It should be noted that phagophores were never seen to contain HRP even after 120-min incubations (Fig. 3 K). We concluded from these experiments with HRP that both Type I and Type II autophagic vacuoles, defined by morphological criteria, are part of the late endocytic pathway and secondly that the kinetics of delivery of HRP confirms that the structures we had classified as Type I autophagic vacuoles do indeed precede Type II autophagic vacuoles on the endocytic pathway. Im-

munocytochemical data to be discussed below provided further validation of the latter conclusion.

The endocytosis of proteins in coated vesicles and their delivery to early endosomes does not depend upon intact microtubules, but the subsequent transport of the endocytosed molecules to late endosomes and lysosomes is dependent on microtubules (Gruenberg et al., 1989). We therefore used low temperature and nocodazole treatment to depolymerize the microtubules in experimental pancreatic lobules and compared the uptake of HRP with that in lobules with intact microtubules. We found that peripheral endosomes contained HRP regardless of the state of the microtubules, but in the absence of microtubules HRP did not reach Type II autophagic vacuoles and only very rarely reached Type I autophagic vacuoles during 90 min continuous incubation with tracer (data not shown). We conclude that transport of HRP from early endosomes to Type I and then Type II autophagic vacuoles depends on intact microtubules.

During these experiments, we noticed that duct lining cells and connective tissue cells in the pancreas contained after 5- and 15-min incubations with HRP more labeled early endosomes than the exocrine cells. Secondly, when lobules were incubated for up to 120 min at 18-20°C, no endocytosis of HRP into the exocrine cells could be detected, whereas other cell types in the tissue contained labeled endosomes. Apparently endocytosis in exocrine pancreatic cells is more sensitive to low temperature inhibition than is endocytosis in other cell types in the pancreas and many tissue culture cell lines.

Acid Phosphatase in Autophagic Compartments: Histochemical Evidence

After processing of pancreas from experimental animals for the histochemical reaction for acid phosphatase, and embedding the tissue in epon, we examined serial sections. We failed to identify phagophores containing reaction product either in single or in serial sections. By contrast, all of the Type I autophagic vacuoles contained reaction product in regions surrounding the ICGs (Fig. 4, A and B). In Type II autophagic vacuoles there were also always heavy deposits of reaction product in the lumen, but it was largely excluded from regions occupied by closely packed internal membrane (Fig. 4, D and E), even though antibody to acid phosphatase labeled the stacked membrane (Fig. 4 F). These findings establish that the Type I and Type II autophagic vacuoles,

Figure 1. Morphology of autophagic compartments in epon-embedded tissue. *A*, *B*, and *C* show phagophores that comprise a smooth osmiophilic bounding membrane (*arrowhead*) enclosing portions of the RER. This RER membrane is studded with ribosomes (*arrow*) and encloses usually a single ICG. Phagophores are spherical or ovoid rather than tubular structures. Note in *C*, the package of phagophore membrane connected to the phagophore (*arrow*), and, in *A*, cisternae of the RER adjacent to the phagophore. *D* shows a phagophore (*arrowhead*) in close proximity to a Type I autophage vacuole (*arrow*), as well as several cisternae of the RER. *E* shows a Type I autophagic vacuole containing several ICGs (*arrowheads*) that have low contrast because this section was contrasted with lead citrate but not with uranyl acetate. Note multilayered membrane material in a surface region (*arrows*) and a single bounding membrane in another region (*small arrow*). Also note the beginnings of accumulation of internal membrane. *F* shows the contents of a phagophore (*arrow*) comparable to those shown in *A* through *C*, within a Type I autophagic vacuole containing other ICGs and whorls of internal membrane (*arrowheads*). *G* shows a Type II autophagic vacuole with ICGs in the lumen (*arrows*) and much internal membrane, parts of which are in stacked parallel arrays. *H* and *I* show at higher magnification the surface regions marked by arrowheads in *G*. As *H* and *I* reveal there appears to be continuity between the bounding membrane of the Type II autophagic vacuole and at least some elements of the internal membrane. *J* shows another example of apparent continuity between bounding an internal membrane (*arrowheads*) in another Type II autophagic vacuole. Bars, 200 nm.
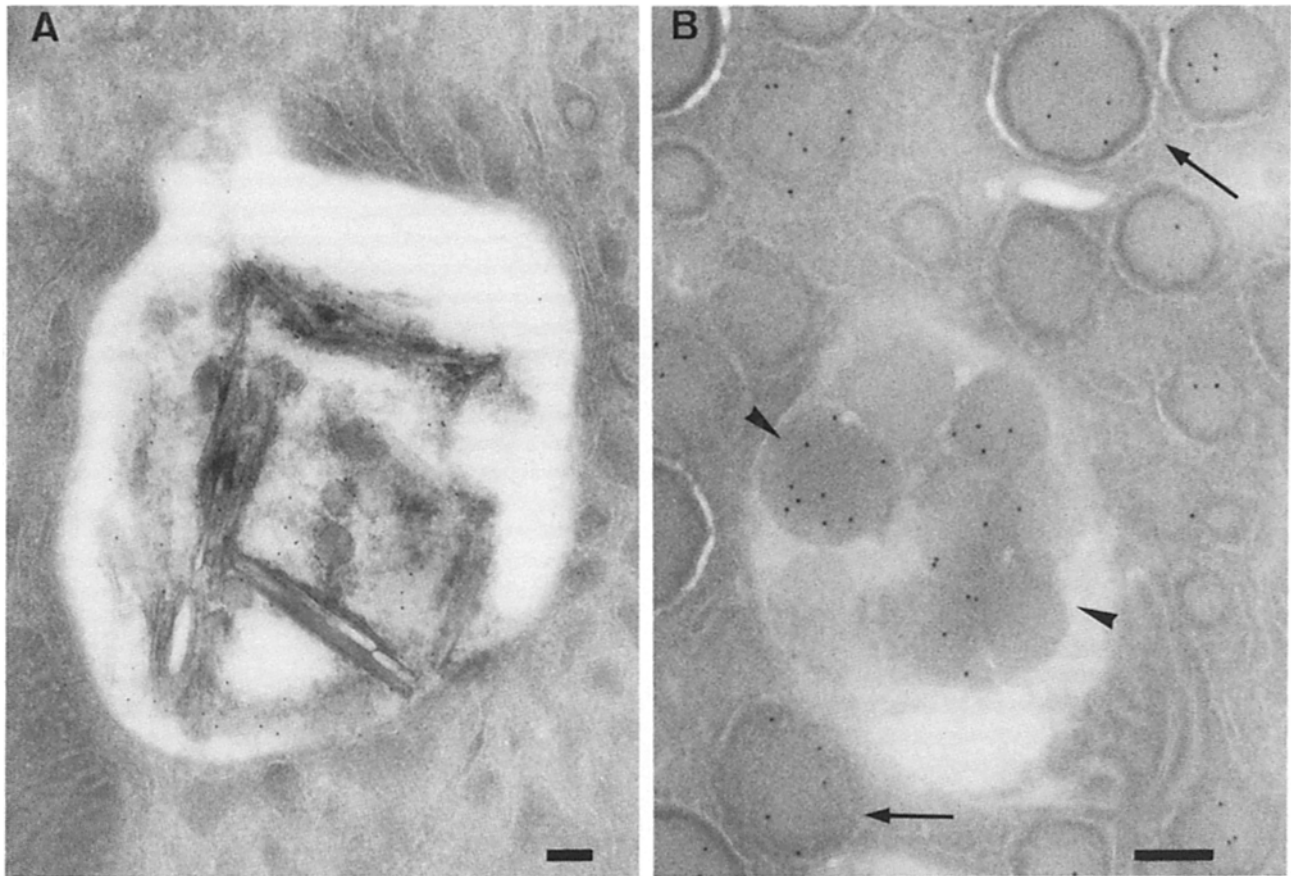
Figure 2. DAMP and chymotrypsinogen labeling of autophagic vacuoles. *A* shows, after incubation with DAMP and labeling with anti-DAMP antibody, a Type II autophagic vacuole labeled significantly above background. Both Type I and Type II autophagic vacuoles were labeled by DAMP and therefore were acidic. *B* shows a cryosection labeled with antibody against chymotrypsinogen. ICGs within both the RER (*arrows*) and an autophagic vacuole (*arrowheads*) were labeled. Bars, 200 nm.

which can be regarded as late endosomes (see above), contain acid phosphatase.

Lysosomal Enzymes in Autophagic Compartments

We investigated the presence of lysosomal enzymes in Type I and Type II autophagic vacuoles using immunogold labeling of cryosections. The antibodies against lysosomal enzymes that were available to us were raised in rabbits against

enzymes from species other than the guinea pig. Several of these antibodies failed to cross react with the corresponding guinea pig enzymes, and this restricted the range of antibodies we could use to the following: anti–bovine cathepsin D; anti–rat cathepsins B, D, and H; and anti–human acid phosphatase. The two antibodies against cathepsin D consistently gave heavier labeling than those against cathepsins B and H, and, therefore, we used the former in most of the labeling experiments. To maximize the chances of preservation of

Figure 3. Endocytosed HRP in the autophagic pathway in experimental guinea pigs. *A* shows early endosomes (*arrows*), near the basolateral plasma membrane, that received HRP during a 5-min incubation. *B* and *C* show similar endosomes (*arrows*) after a 15-min incubation with the tracer. A phagophore in *B* (*arrowhead*) does not contain HRP. *D, E, F,* and *G* show Type I autophagic vacuoles (*arrows*) containing both ICGs and endocytosed HRP, after a 30-min incubation with the tracer. Note in *E* a phagophore (*arrowhead*) that does not contain HRP. *H* shows a Type II autophagic vacuole without HRP after a 30-min incubation. Note HRP between the plasma membranes of two cells (*arrow*) and a labeled endocytic compartment (*arrowhead*). *H* shows a Type II autophagic vacuole with internal membrane (*arrowhead*) close to the basolateral membrane (*arrow*) after a 30-min incubation with the tracer. There is no HRP in the Type II autophagic vacuole, but the tracer is present in the intercellular space and in an endosome (*small arrow*). *I* shows an endosome (*arrow*) and a Type II autophagic vacuole (*arrowhead*), both containing HRP after a 60-min incubation with the tracer. In the Type II autophagic vacuole peroxidase reaction product is excluded from the ICGs and the internal membrane. *J* shows another labeled Type II (*arrowhead*) autophagic vacuole containing HRP after a 90-min incubation with tracer. *K* shows Type I (*arrow*) and Type II (*arrowhead*) autophagic vacuoles containing HRP after a 60-min incubation with tracer. A phagophore (*small arrow*) does not contain HRP. In these experiments, we fixed pancreatic lobules immediately after removing them from the medium with HRP. Reaction product therefore filled the intercellular space. The sections shown in *A, D,* and *G* were not contrasted with lead citrate; the other sections shown were contrasted for <30 s. Bar, 200 nm.
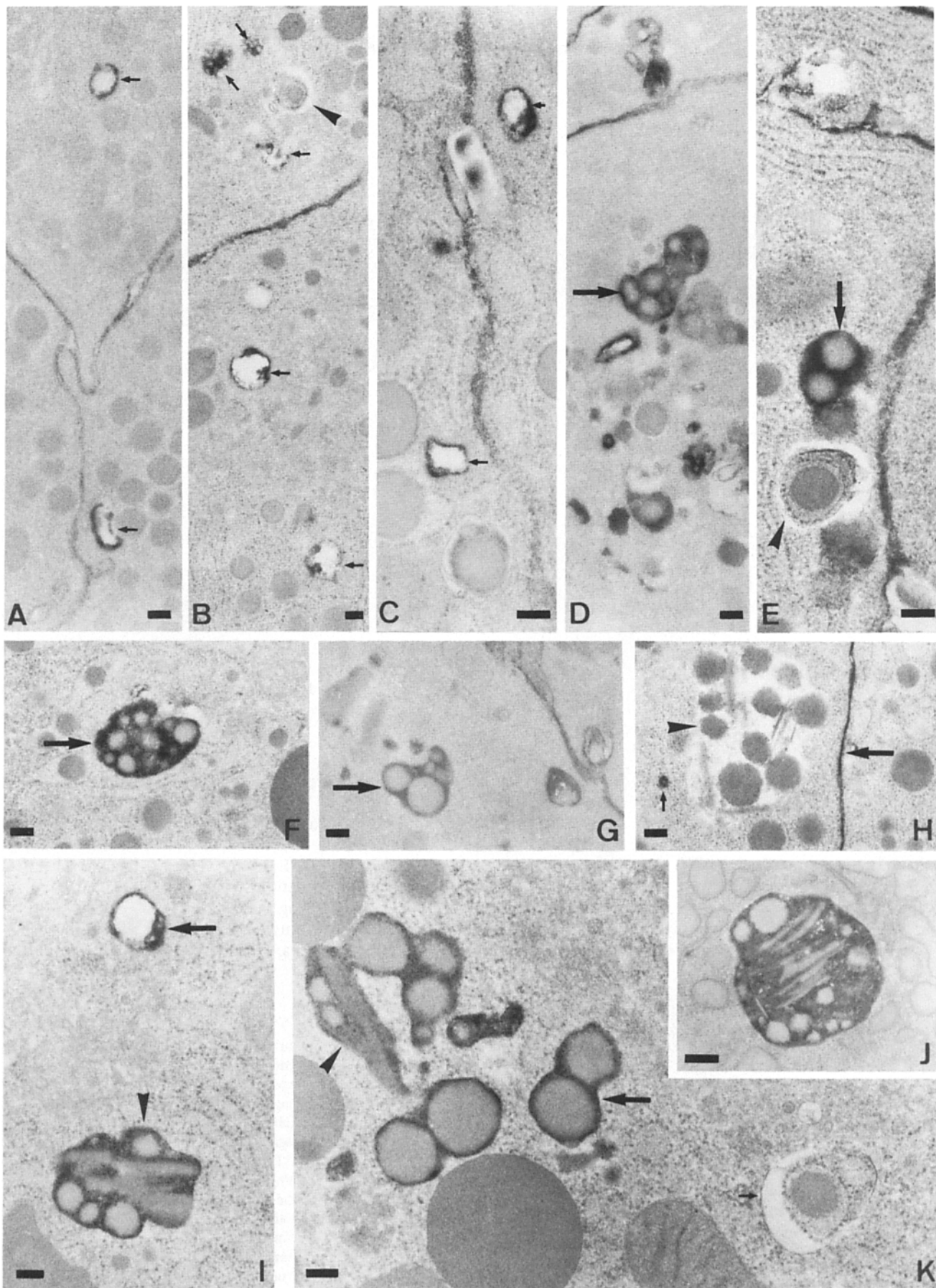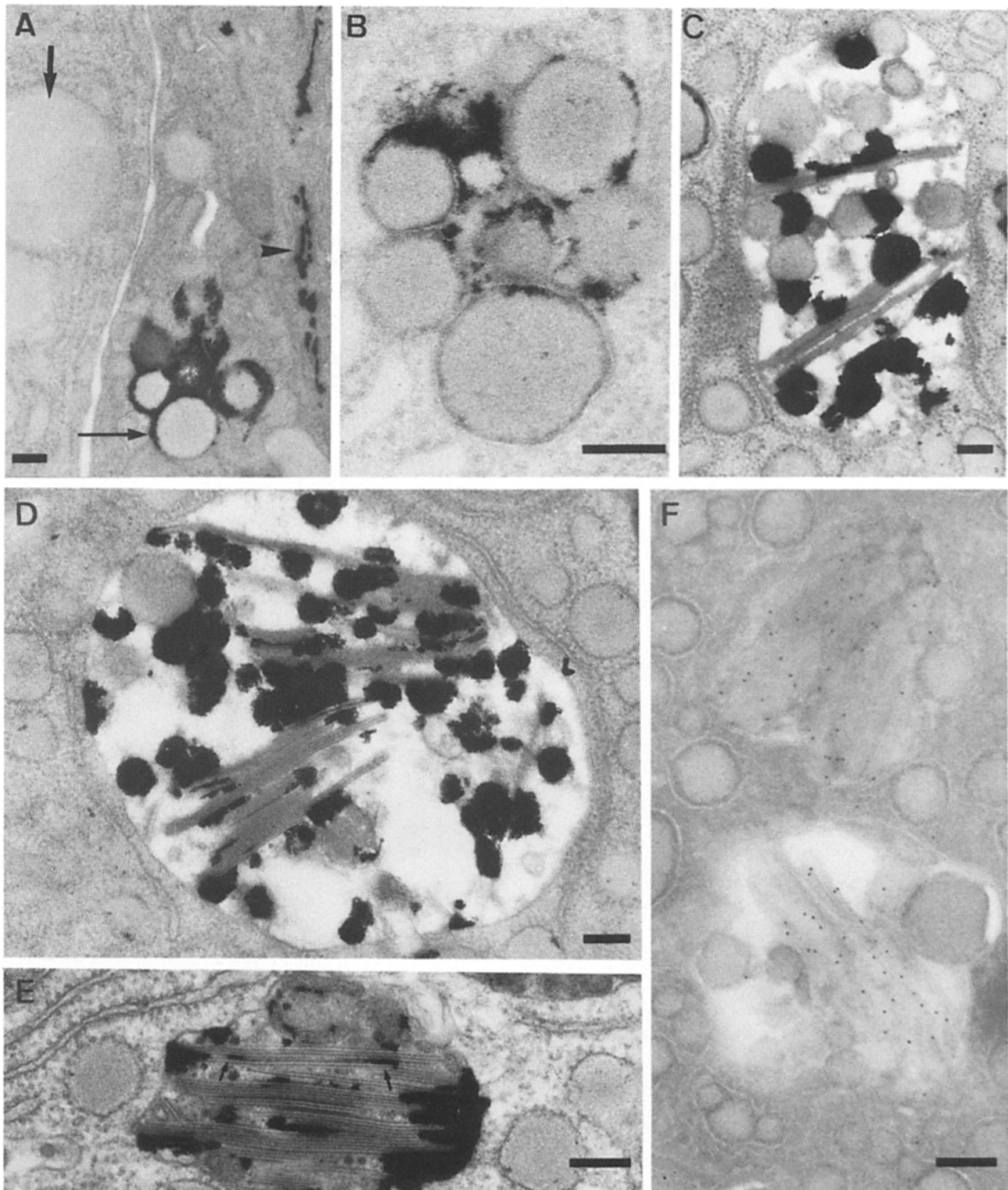
Figure 4. Acid phosphatase in autophagic compartments. *A* shows a Type I autophagic vacuole (*long arrow*) in a cell in the pancreas of a control guinea pig. Acid phosphatase reaction product is seen in the autophagic vacuole and in Golgi cisternae (*arrowhead*). Note the zymogen granule (*short arrow*) in an adjacent cell. *B* shows a Type I autophagic vacuole with characteristic deposition of reaction product in areas not occupied by ICGs. *C* and *D* show Type II autophagic vacuoles with reaction product in the lumen between stacks of internal membrane and around ICGs. (*E*) Rarely, small amounts of reaction product (*arrows*) were seen between the closely opposed sheets of membrane in the stacks, but usually reaction product was excluded from the interior of the membrane stacks. *F* shows the immunogold labeling with antibody against acid phosphatase of Type II autophagic vacuoles in a thin cryo section. Acid phosphatase labeling was present over the stacked internal membrane even though the enzyme could not be detected within the stacked membrane by the histochemical reaction. Bars, 200 nm.

cross-reacting epitopes during fixation, we used fixatives containing only paraformaldehyde and avoided glutaraldehyde fixation. In other words, for the sake of immunoreactivity we sacrificed to some extent morphological preservation.

Phagophores, the least abundant of the three classes of autophagic compartments, were particularly difficult to identify in cryosections, primarily because their characteristic osmiophilic, multilayered membrane could not be resolved in cells not exposed to OsO$_4$. However, the phagophores we managed tentatively to identify (for example, Fig. 5, A inset) were not labeled significantly above background by any of the antibodies against lysosomal enzymes.

In paraformaldehyde-fixed cryosections the morphology of the Type I autophagic vacuoles differed from that seen after conventional glutaraldehyde fixation and epon embedding. Instead of the tight clusters of ICGs surrounded by smooth, often multilayered membrane seen in epon sections, we observed a swollen, distended compartment enclosing numerous ICGs with various amounts of membrane around them (Fig. 5, A and C). Apparently Type I autophagic vacuoles are not well preserved during fixation without glutaraldehyde. In cryosections, these early autophagic vacuoles were lightly labeled with antibody against acid phosphatase (Fig. 5 C); the presence of acid phosphatase was expected from the results of histochemical staining (see above). With antibodies against cathepsin B and D Type I autophagic vacuoles were unlabeled (Fig. 5 A), indicating that other lysosomal enzymes, if present, are at low concentrations below the threshold of detection by immunogold labeling.

By contrast to the Type I autophagic vacuoles, the Type II autophagic vacuoles were relatively well preserved after paraformaldehyde fixation and could readily be identified by virtue of the same morphological characteristics as seen in glutaraldehyde-fixed, epon sections; the differential response of Type I and Type II autophagic vacuoles to paraformaldehyde fixation provides additional, incidental evidence that these two compartments are distinct. All the antibodies against lysosomal enzymes that we used labeled Type II autophagic vacuoles (see, for example, Fig. 5, A–D), and the gold particles were often concentrated over the stacked internal membrane. Using a double labeling procedure with 5- and 9-nm gold, we established that cathepsin and acid phosphatase occur together in late autophagic vacuoles (Fig. 5 D).

After labeling with antibody to acid phosphatase, gold particles were seen over parts of the stacked internal membrane (Figs. 4 F and 5 C) whereas after the histochemical reaction for AcPase, little if any reaction product was seen within the stacked membrane but heavy deposits were present in the lumen (Fig. 4, D and E). We interpret this as showing that the substrate of the histochemical reaction failed to penetrate between the stacked sheets of membrane in the Type II autophagic vacuoles.

As Fig. 5 C exemplifies, in individual thin cryosections of experimental pancreas, we sometimes observed compartments with both the morphological and immunocytochemical features of Type II autophagic vacuoles but lacking ICGs. It is technically impossible to collect serial thin cryosections but we have examined serial sections of epon-embedded tissue (data not shown). This established that when typical Type II autophagic vacuoles containing ICGs are thin sectioned, some individual sections contain no trace of ICGs.

Each thin section ~80-nm thick samples only a small proportion of the total volume of these compartments whose diameters can exceed 1,500 nm. This accounts for images such as Fig. 5 C and for the apparent absence of ICGs from some Type II vacuoles seen in individual thin sections.

Lysosomal Membrane Glycoproteins in Autophagic Vacuoles

An antibody against a lysosomal membrane protein of the rat, anti–lgp120, which heavily labeled rat lysosomes and autophagic vacuoles in cryosections, gave a very low level of immunogold labeling over guinea pig Type II autophagic vacuoles; however, it was specific labeling. Quantitation showed that anti–lgp120 labeling was 10-fold higher over the Type II autophagic vacuoles (4 gold/μm^2) than over all other areas of the cell (0.4 gold/μm^2) in cryosections of pancreas from experimental guinea pigs. We conclude therefore that in both guinea pig and rat pancreas Type II autophagic vacuoles contain lysosomal membrane glycoproteins.

Induction of Autophagy Does Not Alter the Concentration of CI-M6PR

We raised an antibody against CI-M6PR purified from bovine liver. This antibody specifically cross reacts with the CI-M6PR from other species including guinea pigs and rats. To determine whether or not the amount of CI-M6PR changes in guinea pig pancreas after the induction of autophagy of ICGs, we immunoblotted postnuclear supernatants of pancreas and liver from control and experimental animals. The immunoblots were developed with the peroxide reaction and with iodinated protein A (Fig. 6). These experiments, which were repeated with several experimental and control animals, established first that the amount of CI-M6PR in liver and pancreas of guinea pigs was very similar per microgram of total protein, and secondly that the amount of CI-M6PR in the pancreas from experimental and control animals was not detectably different. The induction of autophagy does not, therefore, result in any detectable increase in the amount of CI-M6PR per microgram pancreas protein. Furthermore, blots of fractions from Percoll gradients of control and experimental pancreas showed that the receptor was present in both cases in light fractions at the top of the gradient (data not shown).

Mannose-6-Phosphate Receptor in Autophagic Vacuoles

Having established its specificity by immunoblotting (see above), we used our antibody against bovine CI-M6PR to immunogold label cryosections of guinea pig pancreas. In addition, we labeled cryosections with three other rabbit antibodies raised respectively against rat, chicken, and a second preparation of bovine CI-M6PR. The pattern of labeling was the same with all these antibodies although there were some differences in the intensity of the labeling.

Phagophores, which are difficult to identify in paraformaldehyde-fixed cryosections, were not labeled (not shown). Type I autophagic vacuoles, which as discussed above have a different morphology in cryosections of paraformaldehyde-fixed tissue than in glutaraldehyde-fixed epon embedded tissue, were not reproducibly labeled above background (Fig. 7, A and B). This compartment, in which the endocytic and
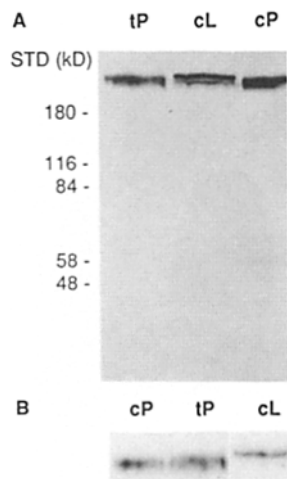
338
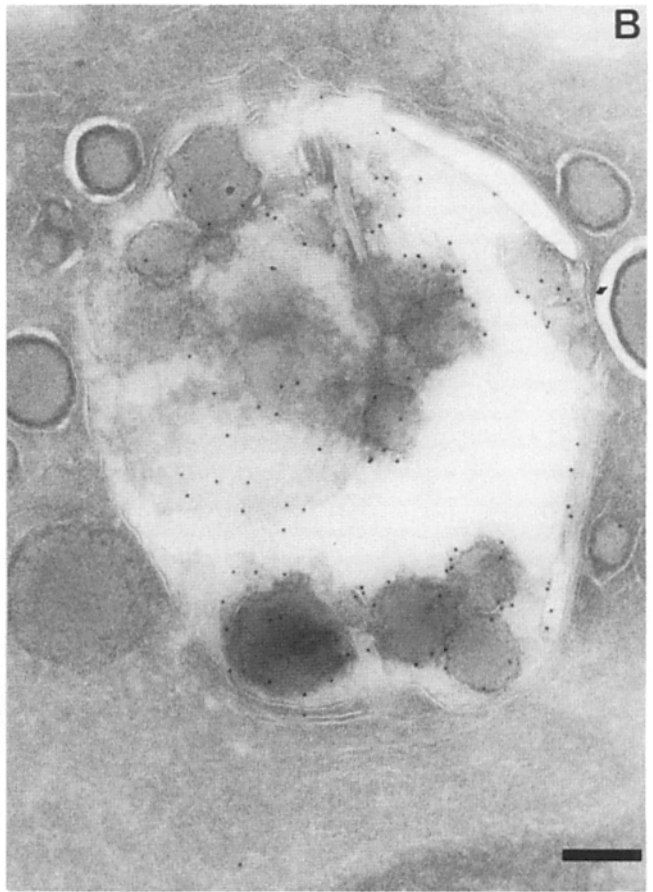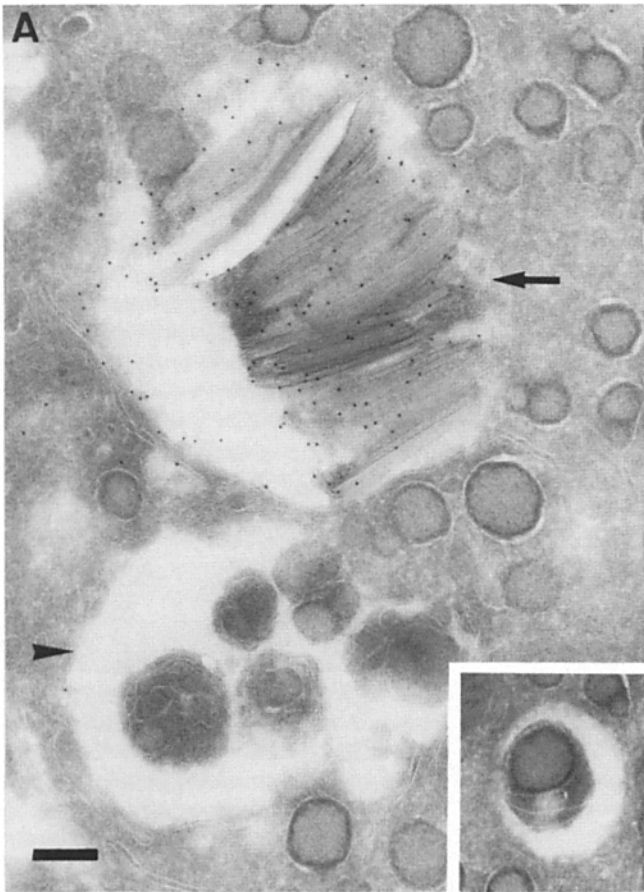
Figure 6. Immunoblot analysis of the CI-M6PR. (*A*) 100 μg of proteins from postnuclear supernatants obtained from pancreas of a treated guinea pig (*tP*) and the liver and pancreas of a control guinea pig (*cL* and *cP*) were separated by SDS-PAGE. After immunoblotting, the CI-M6PR was detected with a second antibody conjugated to peroxidase. (*B*) The same as in *A*, but 50 μg of proteins were loaded on each lane and the CI-M6PR was detected with ^{125}I-protein A.

autophagic pathways first meet is not, therefore, highly enriched for CI-M6PR, although we cannot exclude the possibility that low concentrations of the receptor are present but below the threshold of detection with heterologous antibodies and immunogold labeling.

By contrast, the type II autophagic vacuoles were always very heavily labeled by all four CI-M6PR antibodies (Fig. 7, *A–C*); preimmune serum did not label any compartments in the cells (not shown). Often many of the gold particles were found over the internal membrane of these compartments with comparatively little label associated with the bounding membrane. This remarkable pattern of labeling of CI-M6PR was also seen in prelysosomes in NRK cells (Griffiths et al., 1988). The very extensive labeling of the Type II autophagic vacuoles indicates that, during autophagy, CI-M6PR becomes concentrated in these structures. As expected, double labeling with antibodies against CI-M6PR and lysosomal enzymes confirmed that both were present in the same Type II autophagic vacuoles (Fig. 7 *B*).

The immunoblots of postnuclear supernatants from pancreas (see Fig. 6) showed that the amount of CI-M6PR in control and experimental guinea pigs was essentially the same. However, when we labeled cryosections of control pancreas with the antibody against bovine CI-M6PR used for Western blotting, as well as with the three other antibodies against the receptor, we could not detect any compartments that were heavily labeled like the Type II autophagic vacuoles in the experimental pancreas. We interpret this as indicating that these autophagic vacuoles contain higher concentrations of CI-M6PR than any compartment in normal pancreas, even though the total amount of CI-M6PR per cell is not higher in the pancreas of experimental animals than controls (Fig. 6).

Type II Autophagic Vacuoles Labeled with Soluble CI-M6PR

Soluble lysosomal enzymes in prelysosomal compartments of the delivery pathway to mature lysosomes carry mannose-6-phosphate monoester residues that are recognized by CI-M6PR. By contrast, lysosomal enzymes in mature lysosomes in most cell types lack mannose-6-phosphate residues (see Kornfeld and Mellman, 1989) which are cleaved off in the lysosome. Previous studies have shown that soluble fragments of the CI-M6PR conjugated to gold particles can be used to visualize by cryoelectron microscopy newly synthesized lysosomal enzymes carrying mannose-6-phosphate residues (Ludwig, T., G. Griffiths, and B. Hoflack, manuscript submitted for publication). We therefore used the CI-M6PR-gold to label cryosections of experimental guinea pig pancreas. As Fig. 8 (*A* and *B*) shows, the CI-M6PR-gold labeled heavily and specifically the Type II autophagic vacuoles containing stacked internal membrane. By contrast, Type I autophagic vacuoles were either unlabeled or very lightly labeled (Fig. 8 *A*). When the labeling was done in the presence of mannose-6-phosphate, no gold particles above background were seen over the Type II autophagic vacuoles (Fig. 8 *C*). This competitive inhibition by mannose-6-phosphate established the specificity of the labeling with CI-M6PR-gold. We can conclude from these results that the lysosomal enzymes in Type II autophagic vacuoles carry significant amounts of mannose-6-phosphate residues and that these enzymes are, therefore, prelysosomal.

Discussion

We have exploited the induction of very extensive autophagy following the formation of ICGs in guinea pig exocrine pancreas to define more precisely the relationship between the autophagic and endocytic pathways. By purely morphological criteria, we identified three successive autophagic compartments in these cells, namely phagophores (here we follow the terminology of Seglen, 1987), Type I autophagic vacuoles (which exhibit some of the properties of amphisomes as defined by Gordon and Seglen [1988]), and finally Type II autophagic vacuoles. That these compartments are sequential to one another was confirmed both by the kinetics of their

Figure 5. Immunogold labeling of lysosomal enzymes in Type I and Type II autophagic vacuoles. *A* shows a Type I (*arrowhead*) and a Type II autophagic vacuole (*arrow*) in a thin cryosection labeled with antibody against cathepsin D. Note the heavy gold labeling over the internal membrane of the Type II autophagic vacuole and the complete absence of labeling over the Type I autophagic vacuole. Note also the difference in morphology of the Type I autophagic vacuole compared to that seen after glutaraldehyde fixation and epon embedding (see Figs. 1, 3, and 4). The inset shows a phagophore that was not labeled by antibody to cathepsin D. *B* shows another Type II autophagic vacuole labeled with antibody against cathepsin D. *C* shows a Type I autophagic vacuole (*arrowhead*) lightly labeled by antibody to acid phosphatase adjacent to a compartment resembling a Type II autophagic vacuole, although no ICGs are present in this thin section, which is heavily labeled over internal membrane. *D* shows a Type II autophagic vacuole double labeled with antibody against acid phosphatase (9-nm gold) and an antibody against cathepsin D (6-nm gold, *small arrows*). Note in all these micrographs the very low level of background labeling over other areas of the cytoplasm. Bars, 200 nm.

340
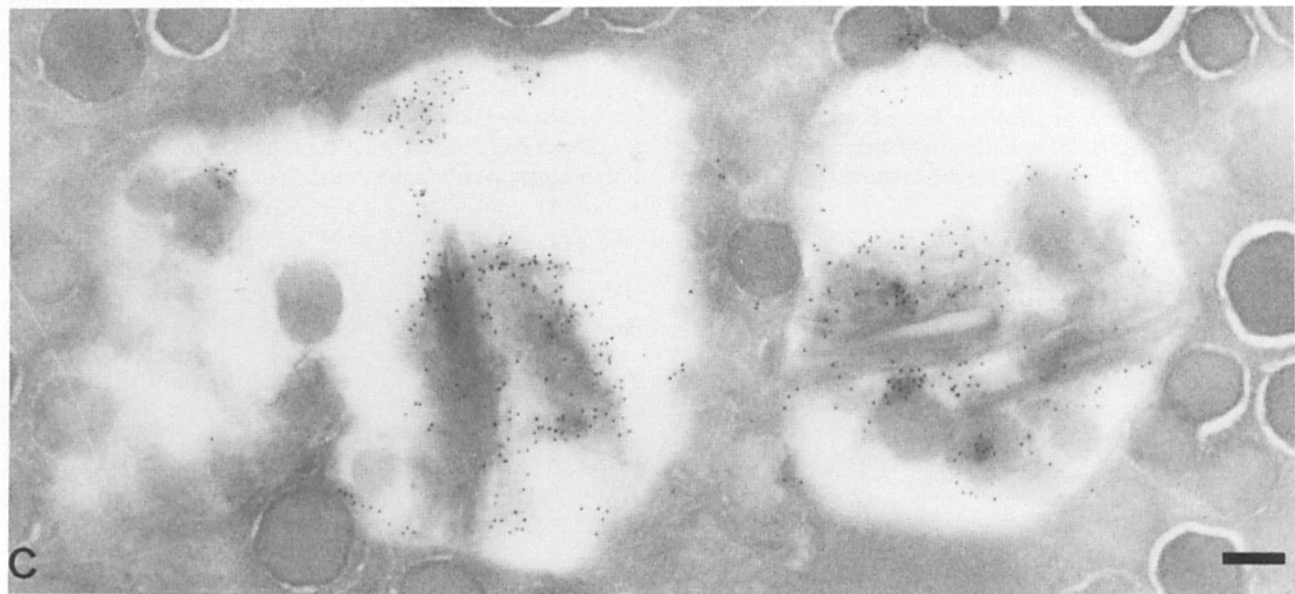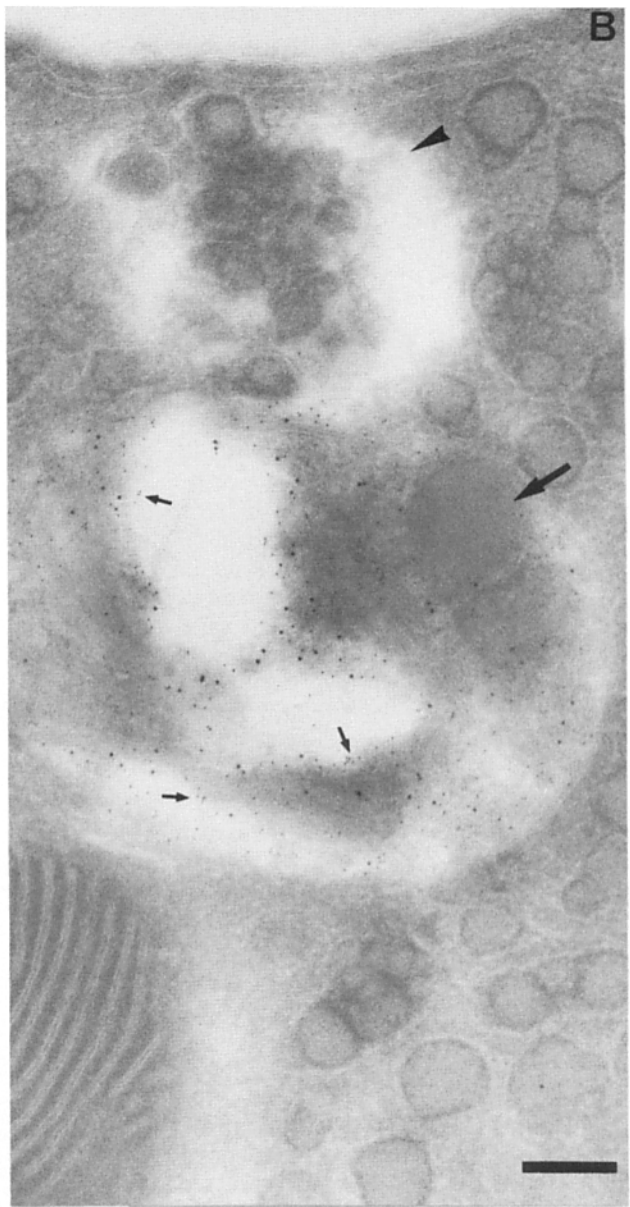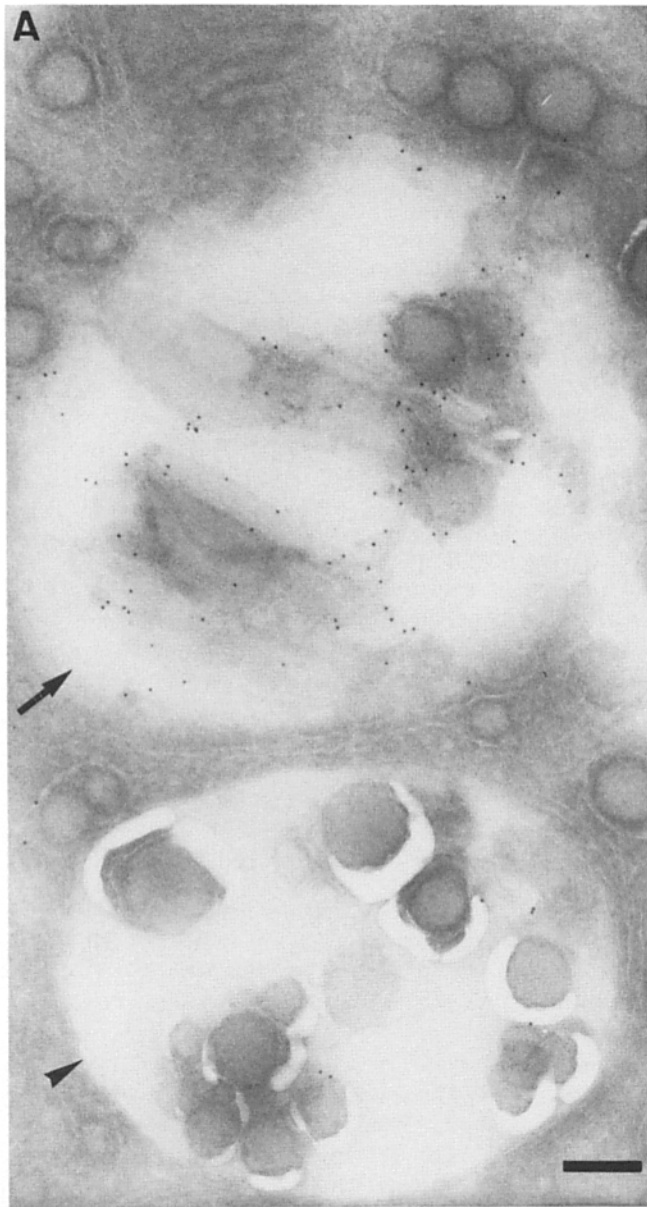
incorporation of endocytosed HRP and by their content of lysosomal proteins as revealed by immunogold labeling.

Many of the micrographs of phagophores in guinea pig pancreas that we obtained are very similar to those of phagophores in rat hepatocytes published by Seglen (1987) who regards the phagophore membrane as a unique organelle with distinctive morphological and biochemical properties. Seglen has suggested that phagophore membrane can envelope and sequester cytoplasm and recycle to and from later autophagic compartments. On the other hand, others interpret electron microscopic observations as showing that the sequestering membrane of autophagic vacuoles is derived from the endoplasmic reticulum or Golgi complex. Clearly the origin, composition and function of the phagophore membrane cannot be defined by electron microscopy alone but will require the isolation of these organelles and their biochemical characterization.

On the other hand, the following pieces of evidence strongly suggest that the function of the phagophore is exclusively sequestration without degradation of the contents of the organelle: first, we failed to find evidence for the presence of acid phosphatase or any other lysosomal enzymes in phagophores; second, phagophores were not labeled by DAMP and by that criterion can be considered to have a neutral pH; and third, the RER within phagophores retains its morphological integrity, whereas in Type I autophagic vacuoles the great majority of ICGs were no longer enveloped in RER and in Type II autophagic vacuoles RER was never observed.

Type I autophagic vacuoles typically contain several ICGs but with rare exceptions (for example, Fig. 1 F) they do not contain RER membrane with bound ribosomes. This indicates that Type I autophagic vacuoles, which contain acid phosphatase, are the first degradative compartments of the autophagic pathway even though they do not have lysosomal characteristics and do not contain the high levels of lysosomal protease and CI-M6PR that are found in Type II autophagic vacuoles. Our results also show that the RER membrane, with bound ribosomes, is degraded much more rapidly than the ICGs, the degradation of which is not completed before they reach Type II autophagic vacuoles. Recent biochemical data have revealed an ER degradative pathway that is independent of lysosomes and very rapidly degrades abnormal proteins in the ER membrane (Lippincott-Schwartz et al., 1988; Chen et al., 1988; Amara et al., 1989; Bonifacino et al., 1990; Wileman et al., 1990). Whether or not this pathway, defined primarily by biochemical experiments, involves phagophores and Type I autophagic vacuoles has still to be determined.

At present, all we can conclude is that those properties of phagophores and Type I autophagic vacuoles that are reported here do not preclude them from being also involved in the novel ER degradative pathway. However, without ki-netic data on the rate of formation of phagophores and the deliver of the sequestered RER to Type I vacuoles, we cannot reach firmer conclusions. Unfortunately, our experimental system, involving the induction of autophagy in vivo over a 3–4-d period, is not well suited for studies of the half-life of phagophores.

How autophaged ICGs move from one compartment of the autophagic pathway to the next is still not fully resolved. From our electron microscopic studies, particularly of serial sections (not shown, but see also Fig. 1, D and F), we feel confident in concluding that phagophores, the smallest and earliest autophagic compartment, fuse with Type I autophagic vacuoles. Indeed, Type I autophagic vacuoles could arise from the fusion of phagophores with each other and with vesicles derived from early endosomes that would deliver endocytosed proteins. Whether Type I vacuoles fuse with Type II vacuoles or mature into them is still unclear. We found no morphological evidence suggesting that ICGs move between these two classes of autophagic vacuoles in carrier vesicles. However, we also failed to detect delivery of endocytosed HRP in transport vesicles from early endosomes to Type I autophagic vacuoles, or the delivery of lysosomal enzymes and CI-M6PR to Type II autophagic vacuoles. It is notoriously difficult to visualize by electron microscopy transport vesicles mediating movement of cargo molecules from one membrane bound compartment to another, and in this respect the autophagic pathway is no exception. In short, while phagophores fuse with Type I autophagic vacuoles, we cannot reach any firm conclusion concerning the step between Type I and Type II autophagic vacuoles.

Convergence of Endocytic and Autophagic Pathways

Our data on the uptake of HRP, a marker of fluid phase endocytosis (Marsh et al., 1986), allow us to draw the following conclusions concerning the convergence of the endocytic and autophagic pathways. First, early endosomes, receiving HRP from the basolateral surface of exocrine pancreatic cells, and phagophores, the first autophagic compartment, do not fuse together and are not in communication via transport vesicles. The initial compartments of the two pathways are distinct. Secondly, endocytosed HRP is delivered from the basolateral early endosomes to the compartment we refer to as Type I autophagic vacuoles concomitant with its delivery to normal late endosomes in the Golgi region of the cell; i.e., between 15 and 30 min after addition of the tracer. Type I autophagic vacuoles are, therefore, a subclass of late endosomes. The presence of acid phosphatase, but at most only very low concentrations of cathepsin D and lysosomal enzymes with mannose-6-phosphate residues, is consistent with this conclusion. Type II autophagic vacuoles, defined by their morphology and the presence of high concentrations

---

Figure 7. Immunogold labeling of CI-M6PR in Type II autophagic vacuoles. *A* shows Type II (*arrow*) and Type I (*arrowhead*) autophagic vacuoles side by side in a thin cryosection. Antibody against chicken CI-M6PR heavily labeled the Type II autophagic vacuole whereas the Type I autophagic vacuole was not labeled above background. *B* shows a Type II autophagic vacuole (*large arrow*) double labeled with antibody against chicken CI-M6PR (9-nm gold) and antibody against bovine cathepsin D (6-nm gold, *small arrows*). Note that the adjacent Type I autophagic vacuole (*arrowhead*) is completely unlabeled by both antibodies. *C* shows two Type II autophagic vacuoles heavily labeled by the antibody against bovine CI-M6PR that was used for the immunoblots shown in Fig. 6. Bars, 200 nm.
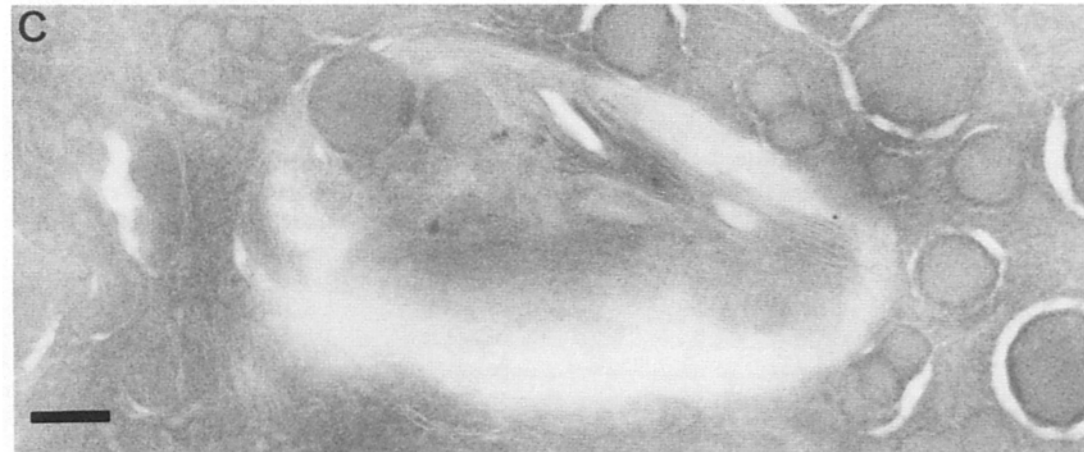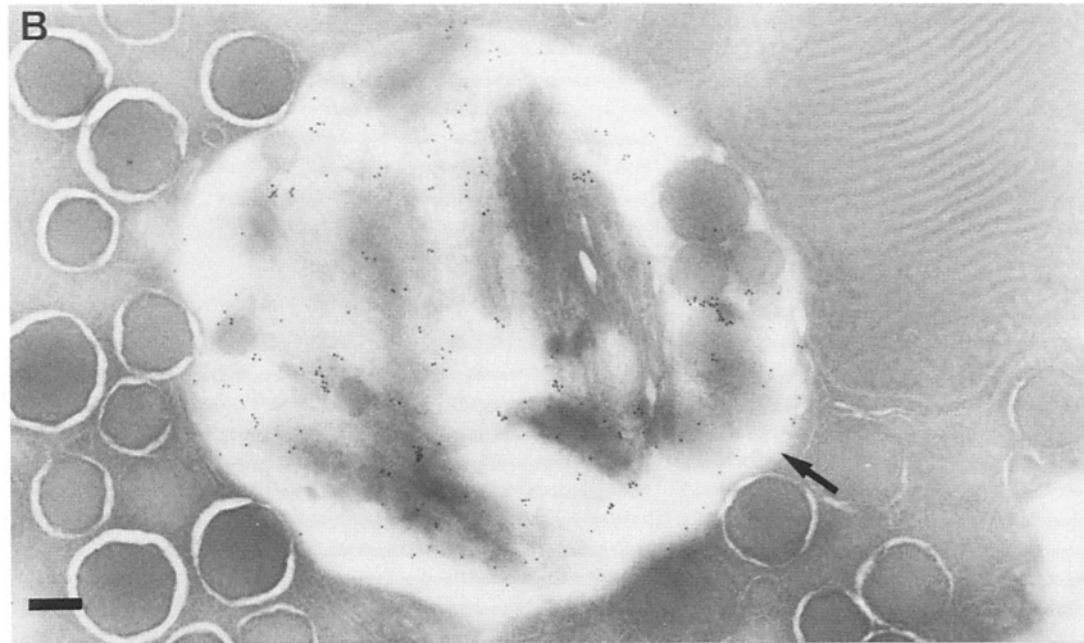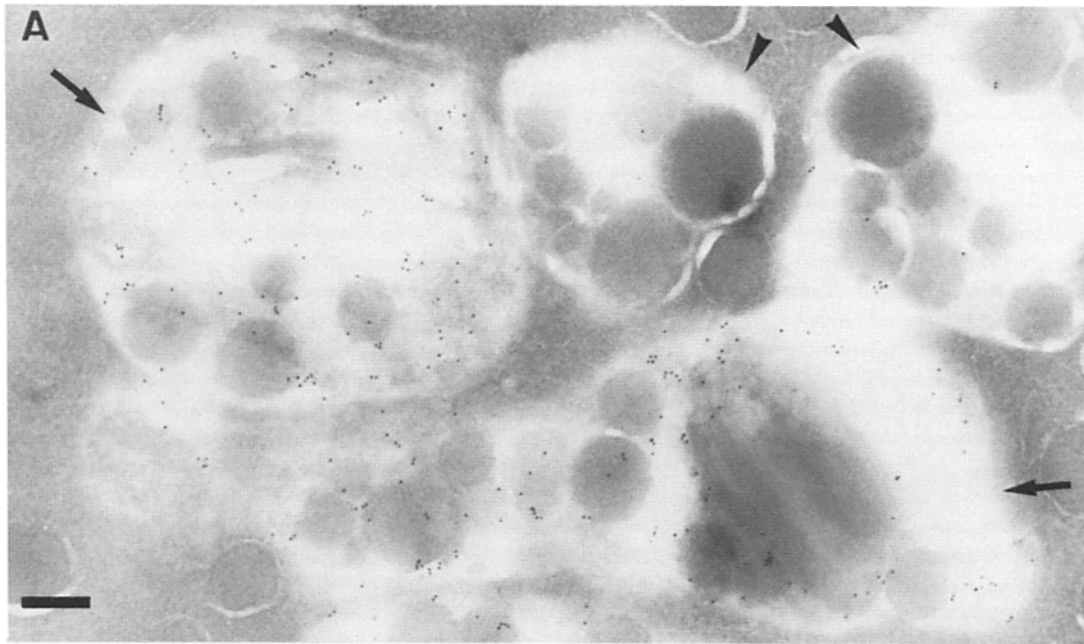
of several lysosomal marker proteins, are clearly later on the endocytic and autophagic pathways than Type I autophagic vacuoles.

In short, the autophagic and the basolateral endocytic pathways converge immediately after the phagophore and early endosome levels. The fact that depolymerization of microtubules in exocrine pancreatic cells prevents fluid phase markers of endocytosis moving from peripheral early endosomes to the two classes of autophagic vacuoles provides additional evidence that the latter are late compartments of the endocytic pathway. Since HRP only reached the apical surface of the polarized exocrine cells after 30 min of incubation, by which time normal late endosomes in the Golgi region of the cell and Type I autophagic vacuoles had received the tracer via the basolateral route, we cannot comment on the relationship between apical early endosomes and the autophagic pathway. Fig. 9 shows a diagrammatic summary of our interpretation of the data discussed above.

Late Autophagic Vacuoles Are Prelysosomes

The morphological characteristics of the Type II autophagic vacuoles, together with the presence of lysosomal membrane glycoproteins and high concentrations of lysosomal enzymes would, in the absence of any data concerning CI-M6PR, lead to the conclusion that these structures are secondary lysosomes. However, it is generally agreed that mature lysosomes do not contain significant amounts of CI-M6PR (for review, see Griffiths et al., 1988; Gruenberg and Howell, 1989; Kornfeld and Mellman. 1989) whereas we have shown here, using four independently raised antibodies against CI-M6PR from three species, that Type II autophagic vacuoles contain very high concentrations of CI-M6PR. If the presence of CI-M6PR is diagnostic of prelysosomes and its absence diagnostic of mature lysosomes, Type II autophagic vacuoles must, by definition, be considered prelysosomal compartments in which the combined endocytic and autophagic pathways have converged with the delivery pathway of lysosomal enzymes.

Type II autophagic vacuoles exhibit all of the diagnostic properties of NRK cell prelysosomes as defined by Griffiths et al. (1988). Both NRK cell prelysosomes and pancreatic Type II autophagic vacuoles appear to contain virtually all the CI-M6PR that can be detected in the cells by immunogold labeling; both are acidic; both contain lysosomal hydrolases and lysosomal membrane glycoproteins; the latter in NRK cells are at very similar concentrations in the membrane of prelysosomes and lysosomes (Griffiths et al., 1990); both receive endocytosed protein and both have extensive arrays of internal membrane with which the CI-M6PR is preferentially associated. Since arrays of internal
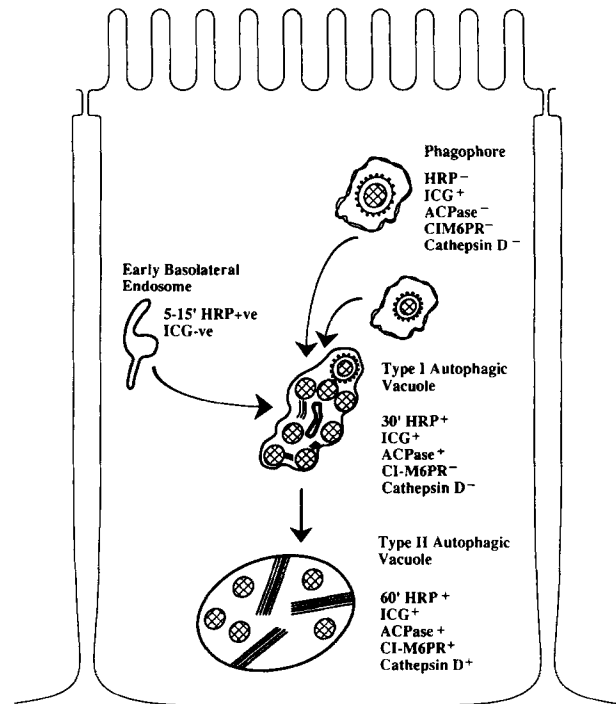

Figure 9. A diagrammatic summary of the convergence of the endocytic, autophagic, and lysosomal enzyme delivery pathways in exocrine pancreatic cells. Early endosomes and phagophores are not in communication. HRP moves from early endosomes to Type I autophagic vacuoles and then to Type II autophagic vacuoles. Type I autophagic vacuoles are a subset of late endosomes. Type II autophagic vacuoles contain lysosomal enzymes and CI-M6PR and are therefore late endosomal prelysosomal compartments.

membrane can be seen in sections of prelysosomes in cells embedded in vitrified water without fixation (McDowall et al., 1989), this internal membrane cannot be a fixation artefact.

According to Griffiths et al. (1988) the prelysosome is penultimate to mature lysosomes, and is postulated to be the compartment from which M6PR, having dissociated from liganded lysosomal enzymes because of the low pH, recycles to the Golgi apparatus. However, in the absence of any direct evidence of such recycling, Kornfeld and Mellman (1989) now regard prelysosomes as a special class of late endosomes that function as intermediates in the late stages of the endocytic pathway to lysosomes. We prefer to retain the term prelysosome (Griffiths et al., 1988), while accepting that prelysosomes may be only a subclass of late endosomes (Kornfeld and Mellman, 1989). Our data show that the au-

---

Figure 8. Type II autophagic vacuoles labeled with soluble CI-M6PR fragments. *A* shows the heavy labeling of Type II autophagic vacuoles (*arrows*) with soluble fragments of bovine CI-M6PR conjugated to 9-nm gold particles. By contrast, adjacent Type I autophagic vacuoles (*arrowheads*) were either unlabeled or very lightly labeled. Type I autophagic vacuoles therefore contain at most only low concentrations of lysosomal enzymes whereas the Type II autophagic vacuoles contain high concentrations of lysosomal enzymes with mannose-6-phosphate residues. *B* shows another example of the heavy and specific labeling of Type II autophagic vacuoles (*arrow*) with soluble fragments of CI-M6PR. *C* shows that mannose-6-phosphate competitively inhibited the labeling of Type II autophagic vacuoles with soluble CI-M6PR fragments. Bars, 200 nm.

tophagic pathway meets the endocytic pathway immediately after the early endosome. After this early convergence of the autophagic and endocytic pathways, the presence of endocytosed and autophaged protein in a compartment with all the hallmarks of a prelysosome is to be expected.

The heavy and specific labeling of Type II autophagic vacuoles with soluble CI-M6PR-gold provides, by a novel technique, compelling evidence that the lysosomal enzymes in these compartments carry mannose-6-phosphate residues. Prelysosomes in NRK cells are also heavily labeled with soluble CI-M6PR-gold (Ludwig, T., G. Griffiths, and B. Hoflack, manuscript submitted for publication). This means that these enzymes cannot have reached the Type II autophagic vacuoles via mature lysosomes. The notion that the presence of lysosomal enzymes in the Type II autophagic vacuoles that we observed results from the fusion of mature lysosomes with an autophagic vesicle is, therefore, ruled out. We should emphasize, however, that we began our studies at a stage when very extensive autophagy of the RER, induced in vivo by a 3-d regime of $CoCl_2$ injections to the animals, was already ongoing. We cannot therefore comment on any events that might be restricted to the period of onset of autophagy and involve preexisting mature lysosomes. This raises a related question, namely are the abundant Type II autophagic vacuoles, enriched in CI-M6PR as well as lysosomal enzymes, the last or the penultimate compartment of the autophagic pathway?

Despite extensive searches of epon-embedded tissue, before and after incubation with HRP, and of immunolabeled cryosections, we failed to identify an additional compartment that was morphologically distinct from Type II vacuoles, contained ICGs, received endocytosed HRP only after long incubations, and contained lysosomal enzymes but not the receptor. If such a compartment exists, it must be very rare to have escaped detection. At least in this experimental system, the Type II autophagic vacuoles appear to be the end point of the degradative pathway of ICGs. Although it is unorthodox to propose that a compartment enriched in CI-M6PR is the terminus of the autophagic pathway and a major location of proteolysis, that conclusion is much more consistent with our findings that the proposal that ICGs are transported from Type II autophagic vacuoles to a later compartment for their final dissolution. In short, we interpret our results as showing that RER membrane and attached ribosomes are degraded in Type I autophagic vacuoles and ICGs in Type II autophagic vacuoles, even though neither of these compartments have the properties expected of classical mature lysosomes. This situation might, of course, be a consequence of the exceptional magnitude of the autophagic load resulting from the massive accumulation of ICGs throughout the lumen of the RER. In such circumstances, it seems conceivable that the final steps in the pathway from prelysosomes–late endosomes to classical mature lysosomes may not take place.

We have shown here by Western blotting that the concentration of CI-M6PR in whole guinea pig pancreas does not increase after the induction of autophagy. However we cannot say whether or not this receptor turns over more rapidly in the experimental animals. Since pancreatic lobules can only be maintained in vitro for a few hours, experiments designed to measure the half-life of CI-M6PR are not feasible. Given that the Type II autophagic vacuoles are highly enriched for the receptor, if it is degraded in these structures then the rate of its synthesis should be increased after induction of autophagy. These uncertainties serve to emphasize that while this experimental system offers advantages for immunocytochemical studies, it is not well suited for biochemical investigations.

Although the findings presented here establish that both CI-M6PR and lysosomal enzymes carrying mannose-6-phosphate residues accumulate in Type II autophagic vacuoles, we still do not know the route by which these proteins are delivered. There are two possibilities, either direct delivery from the *trans*-Golgi network, or delivery via Type I autophagic vacuoles. We were not able reproducibly to label Type I autophagic vacuoles with the available antibodies against CI-M6PR and lysosomal enzymes. However, that may well reflect the fact that all the antibodies we used were raised against proteins from species other than the guinea pig. If our antibodies have a relatively low affinity for the corresponding guinea pig proteins the latter might well escape detection in compartments in which they are at a low concentration. We cannot, therefore, exclude the possibility that at least some lysosomal proteins reach Type II autophagic vacuoles via Type I autophagic vacuoles. Of course, if Type I autophagic vacuoles mature into Type II vacuoles the distinction would be more apparent than real.

Recruitment of Endosomes to Autophagy

We suggest that in normal cells with a basal rate of autophagy exactly the same sequence of events occurs as in the pancreatic cells we have studied. In our view, it is likely, therefore, that some of the prelysosomal compartments in normal cells are involved in autophagy. If the basal rate of autophagy is lower than that in exocrine pancreatic cells containing ICGs, the proportion of prelysosomal compartments with autophaged proteins may be smaller. Moreover without biochemical, morphological, or immunocytochemical markers for autophaged material, a difficulty that the ICGs allowed us to overcome, it is, of course, hard to determine which if any prelysosomes are involved in autophagy.

Our results imply that all compartments of the endocytic-lysosomal pathway after the early endosome have the potential to take part in autophagy and exactly how many of them are called upon to do so depends on the extent of autophagy. As the latter increases, one would expect more of these compartments to be recruited to autophagy while continuing their other functions. Clearly at any one time the proportion of endocytic compartments containing autophaged. but still undigested macromolecules, in our case ICGs, will depend on the rate of delivery and the rates of degradation or export of the latter. In this context it is worth emphasizing that even in guinea pig exocrine pancreas in which high levels of autophagy have been experimentally induced, there are still in the pericentriolar region normal late endosomes that only receive HRP after incubations of longer than 15 min and that do not contain ICGs. In other words, even in these cells not all of the late endosomes appear to have been recruited into the autophagic pathway.

References

Amara, J. F., G. Lederkremer, and H. F. Lodish. 1989. Intracellular degradation of unassembled asialoglycoprotein receptor subunits: a pre-Golgi, nonlysosomal endoproteolytic cleavage. *J. Cell Biol.* 109:3315-3324.

Anderson, R. G. W., and R. K. Pathak. 1985. Vesicles and cisternae in the trans Golgi apparatus of human fibroblasts are acidic compartments. *Cell.* 40:635-643.

Anderson, R. G. W., J. R. Falck, J. L. Goldstein, and M. S. Brown. 1984. Visualization of acidic organelles in intact cells by electron microscopy. *Proc. Natl. Acad. Sci. USA.* 81:4838-4842.

Bonifacino, J. S., C. K. Suzuki, and R. D. Klausner. 1990. A peptide sequence confers retention and rapid degradation in the endoplasmic reticulum. *Science (Wash. DC).* 247:79-82.

Bradford, M. M. 1976. A rapid and sensitive method for the quantitation of microgram quantities of protein utilizing the principle of protein-dye binding. *Anal. Biochem.* 72:248-254.

Burnette, W. N. 1981. "Western Blotting": electrophoretic transfer of proteins from sodium dodecyl sulfate-polyacrylamide gels to unmodified nitrocellulose and radiographic detection with antibody and radioiodinated protein A. *Anal. Biochem.* 112:195-203.

Chen, C., J. S. Bonifacino, L. C. Yuan, and R. D. Klausner. 1988. Selective degradation of T cell antigen receptor chains retained in a pre-Golgi compartment. *J. Cell Biol.* 107:2149-2161.

Geuze, H. J., and J. W. Slot. 1980. Disproportional immunostaining patterns of two secretory proteins in guinea pig and rat exocrine pancreatic cells: an immuno-ferritin and fluorescence study. *Eur. J. Cell. Biol.* 21:93-100.

Gordon, P. B., and P. O. Seglen. 1988. Prelysosomal convergence of autophagic and endocytic pathways. *Biophys. Res. Commun.* 151:40-47.

Griffiths, G., A. W. McDowall, R. Back, and J. Dubochet. 1984. On the preparation of cryosections for immunocytochemistry. *J. Ultrastruct. Res.* 89:65-78.

Griffiths, G., B. Hoflack, K. Simons, I. Mellman, and S. Kornfeld. 1988. The mannose-6-phosphate receptor and the biogenesis of lysosomes. *Cell.* 52:329-341.

Griffiths, G., R. Matteoni, R. Back, and B. Hoflack. 1990. Characterization of the cation-independent mannose-6-phosphate receptor-enriched prelysosomal compartment in NRK cells. *J. Cell Sci.* 95:441-461.

Gruenberg, J., and K. E. Howell. 1989. Membrane traffice in endocytosis: insights from cell-free assays. *Annu. Rev. Cell Biol.* 5:453-481.

Gruenberg, J., G. Griffiths, and K. E. Howell. 1989. Characterization of the early endosome and putative endocytic carrier vesicles in vivo and with an assay of vesicle fusion in vitro. *J. Cell Biol.* 108:1301-1316.

Herzog, V., and H. Reggio. 1980. Pathways of endocytosis from luminal plasma membrane in rat exocrine pancreas. *Eur. J. Cell. Biol.* 21:141-150.

Kern, H. F., and D. Kern. 1969. Elektronenmikroskopische Untersuchungen über die Wirkung von Kobaltchlorid auf das exokrine Pankreasgewebe des Meerschweinchens. *Virchows Arch. Abt. B Zellpathol.* 4:54-70.

Kornfeld, S., and I. Mellman. 1989. The biogenesis of lysosomes. *Annu. Rev. Cell Biol.* 5:483-525.

Lippincott-Schwartz, J., J. S. Bonifacino, L. C. Yuan, and R. D. Klausner. 1988. Degradation from the endoplasmic reticulum: disposing of newly synthesized proteins. *Cell.* 54:209-220.

Marsh, M., G. Griffiths, G. E. Dean, I. Mellman, and A. Helenius. 1986. Three-dimensional structure of endosomes in BHK-21 cells. *Proc. Natl. Acad. Sci. USA.* 83:2899-2903.

McDowall, A., J. Gruenberg, K. Römisch, and G. Griffiths. 1989. The structure of organelles of the endocytic pathway in hydrated cryosections of cultured cells. *Eur. J. Cell Biol.* 49:281-294.

Novikoff, A. B., M. Mori, N. Quintana, and A. Yaw. 1977. Studies on the secretory process in the mammalian exocrine pancreas. I. The condensing vacuoles. *J. Cell Biol.* 75:148-165.

Palade, G. E. 1956. Intracisternal granules in the exocrine cells of the pancreas. *J. Biophys. Biochem. Cytol.* 2:417-422.

Pfeifer, U. 1987. Functional morphology of the lysosomal apparatus. *In* Lysosomes, Their Role in Protein Breakdown. H. Glauman and F. J. Ballard, editors. Academic Press, New York. 3-59.

Scheele, G. A. 1975. Two-dimensional gel analysis of soluble proteins: characterization of guinea pig exocrine pancreatic proteins. *J. Biol. Chem.* 250:5375-5385.

Scheele, G. A., and G. E. Palade. 1975. Studies on the guinea pig pancreas: parallel discharge of exocrine enzyme activities. *J. Biol. Chem.* 250:2660-2670.

Schick, J., H. F. Kern, and G. A. Scheele. 1984. Hormonal stimulation in the exocrine pancreas results in coordinate and anticoordinate regulation of protein synthesis. *J. Cell Biol.* 99:1569-1574.

Seglen, P. O. 1987. Regulation of autophagic protein degradation in isolated liver cells. *In* Lysosomes, Their Role in Protein Breakdown. H. Glaumann and F. J. Ballard, editors. Academic Press, New York. 371-414.

Steinberg, T. H., J. A. Swanson, and S. C. Silverstein. 1988. A prelysosomal compartment sequesters membrane-impermeant fluorescent dyes from the cytoplasmic matrix of J774 macrophages. *J. Cell Biol.* 107:887-896.

Tokuyasu, K. T. 1980. Immunocytochemistry in ultra-thin frozen sections. *Histochem. J.* 12:381-403.

Tooze, J., H. F. Kern, S. D. Fuller, and K. E. Howell. 1989. Condensation-sorting events in the rough endoplasmic reticulum of exocrine pancreatic cells. *J. Cell Biol.* 109:35-50.

Wileman, T., G. R. Carson, M. Concino, A. Ahmed, and C. Terhorst. 1990. The λ and ε subunits of the CD3 complex inhibit pre-Golgi degradation of newly synthesized T cell antigen receptors. *J. Cell Biol.* 110:973-986.